Lethaia
AN INTERNATIONAL JOURNAL OF PALAEONTOLOGY AND STRATIGRAPHY

# Microwear structures and surface analysis on isolated theropod teeth from the Upper Jurassic Andrés fossil site, Pombal, Portugal

FILIPA BATISTA, LÍGIA CASTRO, PATRÍCIA MOITA, BRUNO MAGGIA, FRANCISCO ORTEGA AND ELISABETE MALAFAIA

LETHAIA

The analysis of wear surfaces on teeth has been applied to infer diet, feeding mechanisms, climatic conditions, and habitat in various groups of extinct organisms. Recently, analyses of microwear surfaces have been used to study dinosaur feeding strategies in theropods, demonstrating that different groups may have resorted to similar feeding mechanisms. Here, we present the characterization of wear surfaces and patterns of striations in isolated teeth from Late Jurassic theropods collected at the Andrés fossil site at Pombal, Portugal, based on electron microscopy images. Different morphologies of wear surfaces were identified in the studied sample of isolated teeth. Various origins for these wear surfaces are proposed based on comparisons with dental wear patterns described in other fossil records. Among the identified patterns, the most common may be related to contact between opposing rows of teeth or between the tooth and food, corresponding to wear facets and spalled surfaces, respectively. A particularly pronounced wear surface identified in the sample suggests tooth fracture followed by subsequent wear. Furthermore, correlations between the identified wear surfaces and microstructures with specific habits and feeding mechanisms are explored and tested using Finite Element Analysis. The analysis of these structures holds great potential to enhance our understanding of the palaeoecology of theropod dinosaurs, particularly in inferring dietary strategies. □ *Lusitanian Basin, Coelurosauria,* Allosaurus*, wear patterns, Finite Element Analysis, feeding behaviour*

*Filipa Batista ✉ [fl.batista@campus.fct.unl.pt], Department of Earth Sciences, NOVA School of Sciences and Technology/NOVA FCT, Campus de Caparica, 2829-516 Caparica, Portugal; Lígia Castro [lscastro@fct.unl.pt], Department of Earth Sciences, NOVA School of Sciences and Technology/NOVA FCT and GeoBioTec-pólo FCT-NOVA, Campus de Caparica, 2829-516 Caparica, Portugal; Patrícia Moita [pmoita@uevora.pt], HERCULES Laboratory, Geosciences Department, ECTUÉ, Évora, Portugal; Bruno Maggia [brunomaggia@gmail. com], and Elisabete Malafaia [efmalafaia@ciencias.ulisboa.pt], Instituto Dom Luiz, FCUL Universidade de Lisboa, Lisboa 1749-016, Portugal and Grupo de Biología Evolutiva, Facultad de Ciencias, UNED Universidad Nacional de Educación a Distancia, Avda Esparta s/n, Las Rozas de Madrid, Madrid 2840, Spain; Francisco Ortega [fortega@ccia.uned.es], Grupo de Biología Evolutiva, Facultad de Ciencias, UNED Universidad Nacional de Educación a Distancia, Avda Esparta s/n, Las Rozas de Madrid, Madrid 2840, Spain.;* *manuscript received on 20/11/2024; manuscript accepted on 06/06/2025; manuscript published on 17/11/2025 in* Lethaia *58*(4).

Over the past two decades, various types of tooth wear surface analyses at different scales have been applied to primates and other mammals to infer diet, chewing mechanisms, feeding strategies and food abrasiveness, as well as habitat and climatic conditions (e.g. Rivals & Deniaux 2003; Scott *et al.* 2005; Ungar *et al.* 2007; Schulz *et al.* 2013; Withnell & Ungar 2014; Schulz-Kornas & Winkler 2023). Concerning dinosaur dentition, studies of microwear patterns have primarily focused on herbivorous taxa (e.g. Ősi *et al.* 2014; Skutschas *et al.* 2021; Sakaki *et al.* 2022; Kubo *et al.* 2023). Wear surfaces and microstructures in theropod teeth have been studied by some authors (Farlow & Brinkman 1994; Schubert & Ungar 2005; Candeiro *et al.* 2017) and mentioned by others (Molnar 1998; Ősi *et al.* 2010; Williamson & Brusatte 2014). More recently, Winkler *et al.* (2022) published the first application of dental microwear texture analysis to study theropod feeding ecology, and Torices *et al.* (2018) combined tooth microwear and finite element analyses to demonstrate that different coelurosaurian theropods employed similar puncture-and-pull feeding mechanisms, while differences in denticle morphology may be related to diverse predation strategies.

Recently, several authors have recognized two different types of surfaces related to feeding on theropod tooth crowns: 1) surfaces resulting from repeated tooth-to-tooth contact, which correspond to wear facets; and 2) surfaces formed by interactions

https://doi.org/10.18261/let.58.4.2 

between the teeth and the food, known as spalled surfaces (Schubert & Ungar 2005; Hendrickx *et al.* 2015). According to these authors, wear facets are typically elongated and elliptical in outline and may occur on either lingual or labial side of the crown, but never on both, nor on the mesial and distal surfaces. These facets are usually flat, aligned with the long axis of the crown, and can vary in size from subtle marks to very large surfaces. Wear facets usually exhibit parallel striations and extend well into the dentine. On the other hand, spalled surfaces tend to be shorter, relatively shallower, and irregular in shape, resulting from enamel flaking and extending towards the apex of the tooth. These may occur on all surfaces of the crown, are conchoidal in nature, and can be oriented perpendicular to the long axis of the tooth. In addition to these two surface types, patterns of striations adjacent to the denticles may indicate different feeding mechanisms or food preferences, including the processing of hard material such as bones (e.g. Candeiro *et al.* 2017; Torices *et al.* 2018; Winker *et al*. 2022). Torices *et al.* (2018) focused on the functional significance of denticles morphology in theropod teeth and identified two main directions of scratches near the denticles and carinae, which were interpreted as indicators of a puncture-and-pull feeding movement. A similar feeding mechanism was proposed for other theropods, including *Allosaurus*, based on dental microwear texture analysis (Winkler *et al.* 2022).

Here, the wear surfaces and microstructures of a sample of isolated teeth from different small Late Jurassic theropods collected at the Andrés fossil site are described. Different origins are proposed for the identified wear patterns based on comparisons with those described in other fossil records. Feeding mechanisms are interpreted based on analysis of the described microwear and results of Finite Element Analysis (FEA) performed on the most complete tooth in the sample (MNHN/UL.AND.208). The specimens were previously attributed to different theropod groups (Table 1), including *Allosaurus*, indeterminate Coelurosauria, an early-branching tyrannosauroid, indeterminate Neocoelurosauria, and dromaeosaurids possibly related to Dromaeosaurinae and Velociraptorinae.

## Geological setting

The Andrés fossil site is located in the parish of Santiago de Litém, Pombal (Fig. 1A, B), which lies within the Central Sector of the Lusitanian Basin, a sedimentary basin that developed along the western Iberian margin from the Late Triassic to the Early Cretaceous (Kullberg *et al.* 2013). Andrés is situated in the Mamede sub-basin (Fürsich *et al.* 2022) (Fig. 1C) and the sedimentary levels at the site were first described as belonging to the upper part of the 'Camadas de Alcobaça' unit (Manuppella 1974; Manuppella *et al.* 1978). More recently, these levels have been considered part of the Lourinhã (Fürsich *et al.* 2022) or Bombarral (*sensu* Azerêdo *et al.* 2010) formations, the latter is mostly considered to be Tithonian in age (Fig. 1A, C). The sedimentary levels at the fossil site essentially consist of fine, micaceous sandstones containing coal remains, intercalated with brown and reddish clay lenses. The fine-grained sandstone levels sometimes display parallel lamination, abundant carbonized plant remains, and carbonate concretions (Malafaia *et al*. 2010). Some fine red and grey clay lenses intercalated within the sandstones yielded some freshwater bivalves and gastropods. This sequence laterally transitions into a thick level of massive red mudstones. The facies association identified at the Andrés site indicates a medium- to high-sinuosity fluvial system with multiple channels and crevasse splays on a large floodplain, in which seasonal climatic variations led to repeated flooding and drying episodes (Pimentel 2009; Malafaia *et al.* 2010).

*Table 1.* Taxonomic interpretation of the tooth specimens studied in this work

| Specimen | Tooth position | Taxonomic interpretation |
|---|---|---|
| MNHN/UL.AND.212 | Lateral | Dromaeosauridae indet. (cf. Velociraptorinae) |
| MNHN/UL.AND.26 | Lateral | Dromaeosauridae (cf. Dromaeosaurinae) |
| MNHN/UL.AND.213 | Mesial | Coelurosauria indet. |
| MNHN/UL.AND.206 | Lateral | *Allosaurus* (juvenile) |
| MNHN/UL.AND.208 | Lateral | Dromaeosauridae (cf. Velociraptorinae) |
| MNHN/UL.AND.209 | Mesial | Neocoelurosauria indet. |

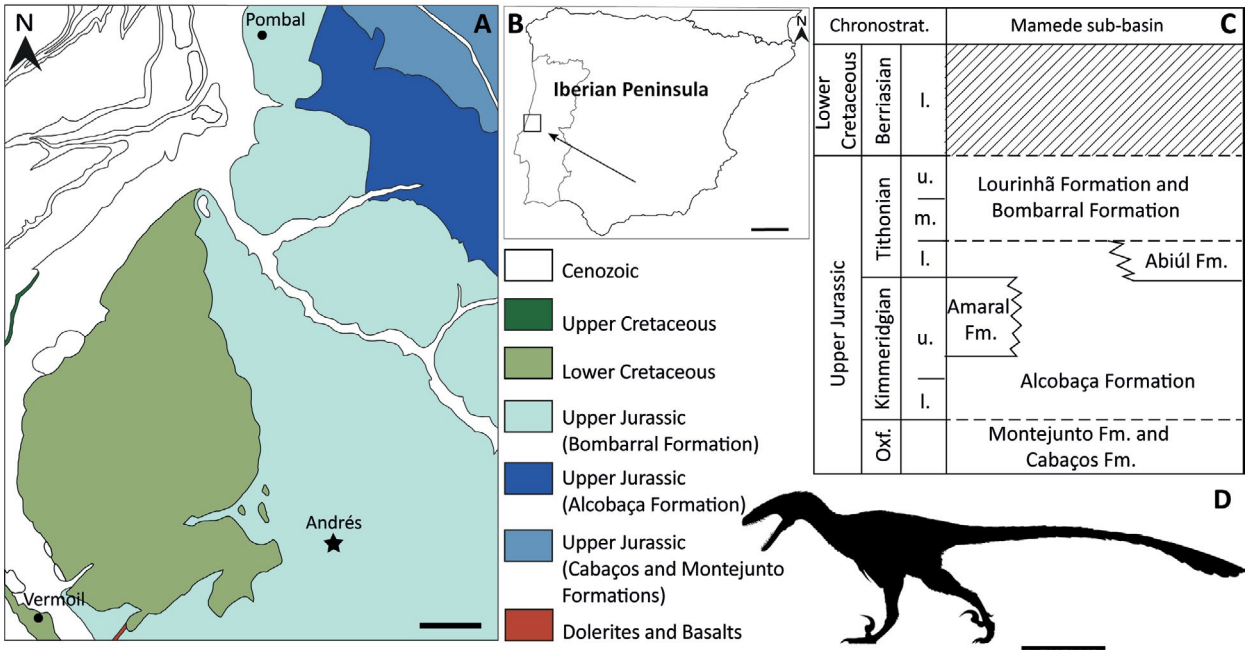


*Fig. 1.* Geological context of Andrés and stratigraphical context of the Mamede sub-basin. A, geological map of the region of Andrés (modified from Manuppella, 1974). B, geographical location of the fossil site (Upper Jurassic of Pombal) in the Iberian Peninsula. C, simplified stratigraphy of the Upper Jurassic sequences in the region of Andrés, based on Malafaia *et al.* (2024). D, dromaeosaurid silhouette (downloaded from phylopic.org; artist: Scott Hartman). Scale bars: 3 km (A), 150 km (B), 50 cm (D).

## Taphonomic aspects of the site

The Andrés fossil site displays a complex taphonomic signature, indicative of a dynamic fluvial floodplain environment characterized by fluctuating energy regimes and variable depositional conditions. The preservation of both large, occasionally articulated vertebrate remains (notably *Allosaurus*) and abundant small vertebrate fossils, such as fish scales, small theropod teeth, crocodyliforms, and sphenodontians points to a multiphase taphonomic history (Dantas *et al.* 1999; Pérez-Moreno *et al.* 1999; Malafaia *et al.* 2010). This likely involved transport and sorting, where the fine-grained nature of the sediments and the concentration of isolated small vertebrate fossils within clay lenses suggesting deposition in low-energy settings (e.g. overbank deposits or abandoned channel fills). Larger vertebrate remains, including the orientation of certain elongated *Allosaurus* bones (Malafaia *et al.* 2010), indicate a prevailing E–W palaeodrainage at the site. The presence of abundant carbonate concretions, frequently associated with skeletal remains – such as a large concretion preserving elements of the pelvic girdle and hindlimb of *Allosaurus* in anatomical position – suggests early diagenetic processes associated to the decay of soft tissues (Malafaia *et al.* 2010).

## Material and methods

The studied material consists of a sample of six isolated theropod teeth (MNHN/UL.AND.213, MNHN/UL.AND.26, MNHN/UL.AND.208, MNHN/UL.AND.212, MNHN/UL.AND.209, MNHN/UL.AND.206), from the Upper Jurassic of the Andrés fossil site. These teeth were collected during various excavation campaigns conducted between 2005 and 2010. They are housed in the palaeontological collections of the Museu Nacional de História Natural e da Ciência (National Museum of Natural History and Science) in Lisbon and are catalogued under the reference MNHN/UL.AND# (MNHN/UL denotes Museu Nacional de História Natural e da Ciência/Universidade de Lisboa; AND refers to Andrés; and #, corresponds to the element number).

For the study of the tooth wear structures, the specimens were first observed and photographed using a Phenom ProX Generation 5 Scanning Electron Microscope (SEM), equipped with an integrated Energy Dispersive Spectrometer (EDS) and a Backscattered Electron Detector (BSD). Images were taken at an accelerating voltage of 10 kV. To obtain higher-resolution images and to observe more specific details on some crowns, a HITACHI™ S3700N SEM, coupled with a Bruker™ Xflash 5010 SDD EDS detector, was

also used. These analyses were conducted under partial vacuum conditions (40 Pa), with an accelerating voltage of 20 kV and a working distance of 10 mm between the detector and the sample. Photographs were taken using the BSD detector, which provides chemical contrast information, thereby enhancing detailed observation. The images focused on the wear surfaces (when present), their textures and structures, as well as on scratches and striations associated with the denticles.

A comparison between the wear structures observed in the specimens from Andrés and patterns described in the literature was carried out to infer the possible origin of these surfaces and scratches, considering their orientation and relative abundance. For this analysis, the methodology largely followed that outlined by Torices *et al.* (2018). However, it was not possible to measure the orientation of one hundred scratches relative to the carina. Instead, an attempt was made to measure eighty striations per tooth. The mean orientation value and standard deviation were calculated for each specimen. The formula for circular mean values (Fisher 1993; Paula & Carvalho 2024) was used to calculate the mean angle, which is expressed as:

$$\overline{\theta} = atan2(\overline{y}, \overline{x}),$$

Where, for each $\theta_i$, the corresponding unit vector components are given by:

$$x_i = \cos(\theta_i),\ y_i = \sin(\theta_i),$$

and the average of the $x_i$ and $y_i$ components is:

$$\overline{x} = \frac{1}{n}\sum_{i=1}^{n} x_i,\ \overline{y} = \frac{1}{n}\sum_{i=1}^{n} y_i$$

If the angles are in degrees, they must be converted into radians before applying these formulae and once the mean value is obtained, the result is converted back into degrees.

The formula used to calculate the circular standard deviation (Paula & Carvalho 2024) is expressed as:

$$\sigma = \sqrt{-2\ln(R)},$$

where $R$ is the length of the mean resultant vector ($R = \sqrt{\overline{x}^2 + \overline{y}^2}$).

The scratches were measured on the apical part of the crowns, where they are most commonly found. Some specimens were excluded from these statistical analyses because the number of identified striations was fewer than eighty.

A 3D model of a dromaeosaurid tooth (MNHN/UL.AND.208) was generated using images acquired with a SkyScan 1172 microtomographer (Bruker micro-CT), equipped with a Hamamatsu 100/250 source and a VDS 1.3 Mp camera. Rendering images were produced at a resolution of 6.70 × 6.70 × 6.70 µm, using the free SkyScan software CTVox, varying the colour transfer function curves and adjusting the lighting and shadowing options. The 3D model was obtained by generating a contour mesh in Dragonfly 3D World (version 2024.1). Damaged denticles and minor defects in the model were repaired in Blender 3.6, after which the model was cleaned and converted to meshes in Geomagic Wrap and ANSYS. The final mesh of the model was approximately 721 000 elements. Following previous studies (e.g. Lautenschlager *et al.* 2013, 2016; Lautenschlager, 2017), the mechanical properties of *Alligator mississippiensis*' enamel ($E$ = 60.40 GPa, $\upsilon$ = 0.31), as measured by Creech (2004), were applied to the mesh in ANSYS. Constraints were placed at the base of the tooth, and a force of 90 N, corresponding to the estimated bite force for Velociraptorinae, based on comparison with *Varanus komodoensis* (Therrien *et al.* 2005; Moreno *et al.* 2008), was applied and distributed along the denticles of the distal carina. Following the methodology described by Torices *et al.* (2018), different cutting angle scenarios were tested, by applying the force at 0°, 15°, 30°, 45°, 60° and 75° (Fig. 2). Additionally, a

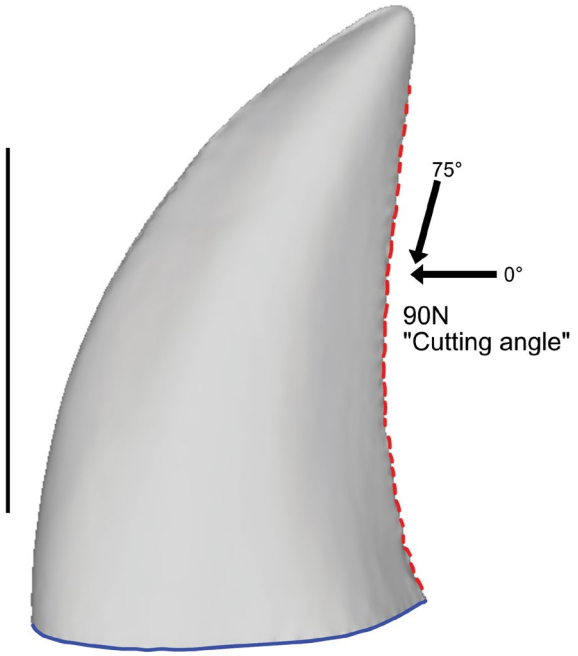


*Fig. 2.* Free body diagram of the Dromaeosauridae (cf. Velociraptorinae) tooth (MNHN/UL.AND.208) with the areas where the forces were applied in red and the constraint in blue. The arrows represent the different directions of the applied forces for the cutting angles of 0° and 75°. Scale bar: 3 cm.

*Table 2.* Orientation of the oblique scratches, with the maximum, minimum and mean value of the measured angles, as well as the standard deviation obtained for each tooth. For the mean value and standard deviation there are the results obtained with both linear and circular formulae. The asterisk symbol (*) indicates specimens for which the eighty measures were not possible to take

| Specimen | Max. | Min. | Mean | | Standard Deviation | |
|---|---|---|---|---|---|---|
| | | | Linear | Circular | Linear | Circular |
| MNHN/UL.AND.213 | 82° | 10° | 37° | 37° | 17,88 | 17,82 |
| MNHN/UL.AND.26 | 82° | 10° | 36° | 35° | 19,01 | 18,95 |
| MNHN/UL.AND.208 | 88° | 16° | 55° | 55° | 18,09 | 18,02 |
| MNHN/UL.AND.212* | 91° | 28° | 55° | 45° | 16,98 | 16,59 |
| MNHN/UL.AND.209* | 63° | 13° | 34° | 34° | 20,34 | 19,54 |
| MNHN/UL.AND.206* | 55° | 10° | 22° | 22° | 11,46 | 11,28 |

55° angle scenario was included, corresponding to the average orientation of the oblique scratches measured for MNHN/UL.AND.208 (see Table 2).

# Results

## *Description of wear surfaces and microwear structures*

*MNHN/UL.AND.212.* – This specimen was interpreted as a lateral crown attributed to Dromaeosauridae, possibly related to a velociraptorine (Malafaia *et al.* in review) (Table 1). It has a well-developed wear surface that begins at the tooth apex and extends to approximately mid-height of the labial surface of the preserved crown (Fig. 3A, B). The apical end appears worn and displays a fractured border, whereas the remaining margins are mostly regular. The wear surface is oval in shape, with its long axis being mostly parallel to the mesial margin of the crown (one of its borders coincides with the mesial margin of the crown). In some parts of the wear surface, the dentine is exposed (Fig. 4). Although part of the surface is covered by sediment, there are some visible striations within the wear facet that are parallel to the long axis of the wear surface. Inside the wear surface, near its border on the labial surface, there are two smaller, apicobasally elongated concavities adjacent to each other that could be smaller secondary wear surfaces. Although sediment partially covers these smaller surfaces, making it difficult to verify the possible presence of additional wear structures, it is evident that their orientation follows the long axis of the main wear surface. On the lingual side of the tooth crown, a second and smaller wear evidence is present (Fig. 3C, D). It is a semi-circular surface located at the apical part of the lingual surface, that appears to be less deep and it is entirely covered by sediment, preventing the observation of any scratches or other patterns. The borders of this surface are more irregular than those of the wear surface on the labial side.

Striations were identified on the apical and central denticles of the distal carina (Fig. 3E, F). Although a few parallel scratches are present, most of them are oriented perpendicular or oblique to the crown's distal carina. The perpendicular scratches are generally wider and deeper than the oblique ones. Towards the base of the crown, striations adjacent to the denticles are smaller and less frequently observed, which may be due to sediment covering the surface. No striation pattern was identified on the basal denticles.

*MNHN/UL.AND.26.* – This specimen was interpreted as a lateral crown attributed to a possible dromaeosaurid (Malafaia *et al.* in review) (Table 1). A large wear surface extends from the apex to at least 5 mm along the mesial margin of the crown, affecting both the labial and lingual surfaces (Fig. 5A–C). Another wear surface extends along the distal carina, where the apical denticles are worn down, but only on the labial side of the crown. This forms a conchoidal surface that is filled with sediment. On the large wear surface, some parallel scratches (i.e. following the direction of the mesial margin of the crown) are present, along with perpendicular and a few oblique striations. These features are visible only on the most apical part of the wear surface, as the surface is covered by sediment towards the mesial margin.

The most apical denticles of the mesial carina are almost completely abraded, and in their place are small concavities filled with sediment. As a result, only small denticles are visible along the mesial margin of the crown, just below the end of the wear surface (Fig. 5D). These denticles display several parallel and oblique striations on their surface and near the base. In general, the length of these striations tends to increase towards the apex of the crown. No other wear patterns were identified in association with the mesial denticles, as their surfaces are mostly covered

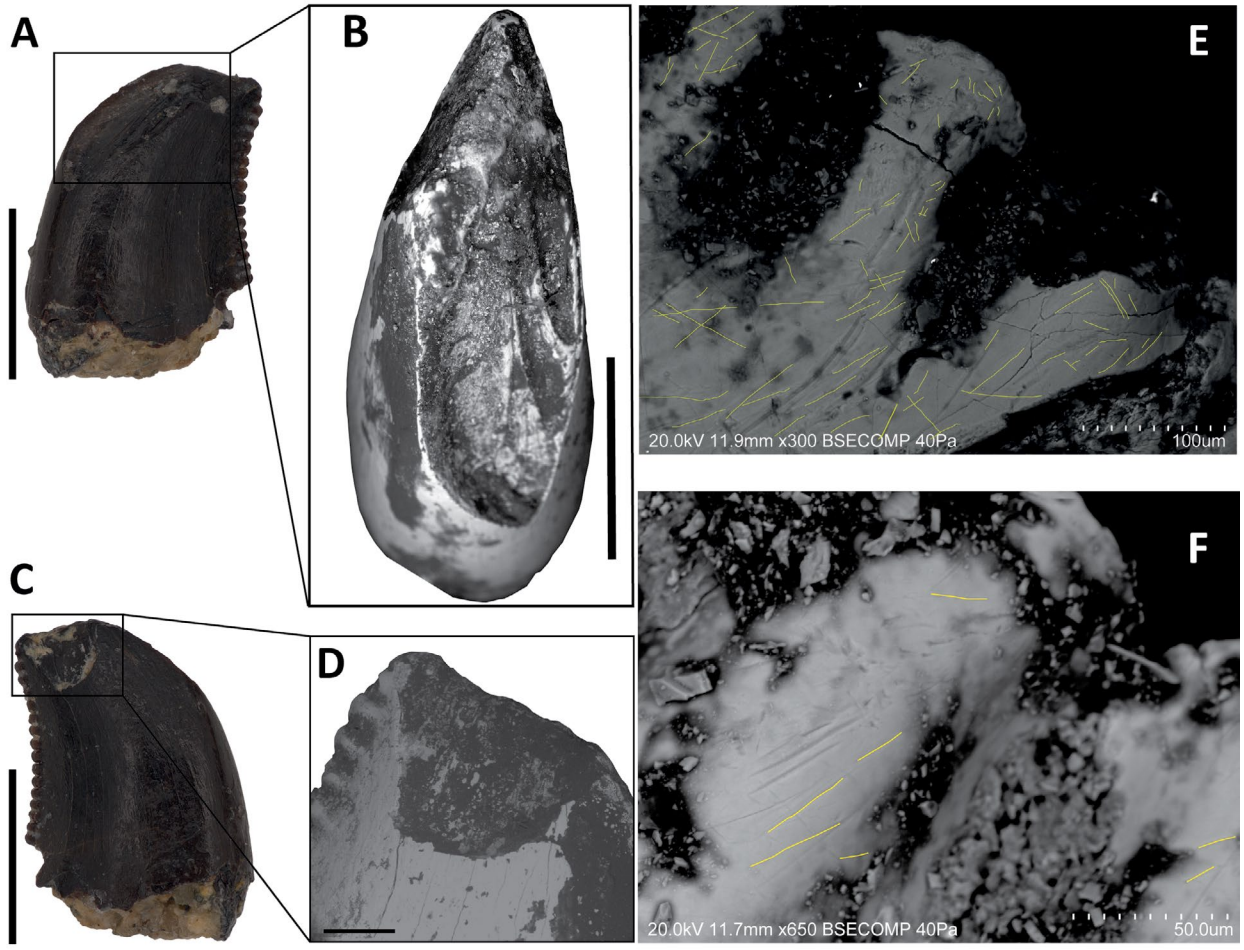


*Fig. 3.* Specimen MNHN/UL.AND.212. A, crown in labial view. B, detail of the wear surface in apicomesial view on the SEM. C, crown in lingual view. D, detail of the spalled surface in apicolingual view on the SEM. E, detail of the scratches on the apical distal denticles on the SEM. F, detail of the scratches on the central distal denticles on the SEM. Scale bars: 2 mm (A, C), 1 mm (B), 300 μm (D).

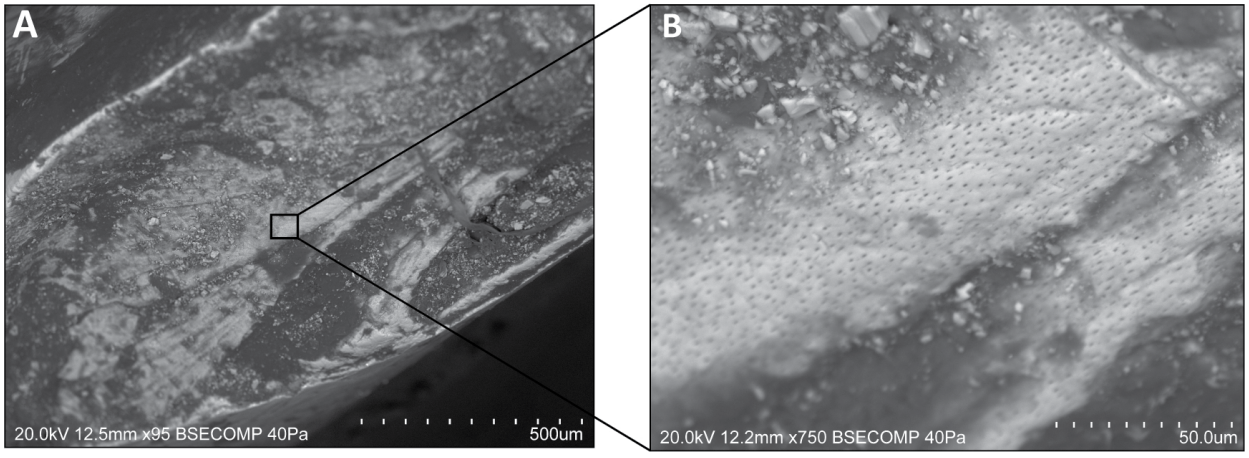


*Fig. 4.* Wear surface on MNHN/UL.AND.212. A, detail of the labial wear surface on the SEM. B, detail of the dentine seen within the surface on the SEM.

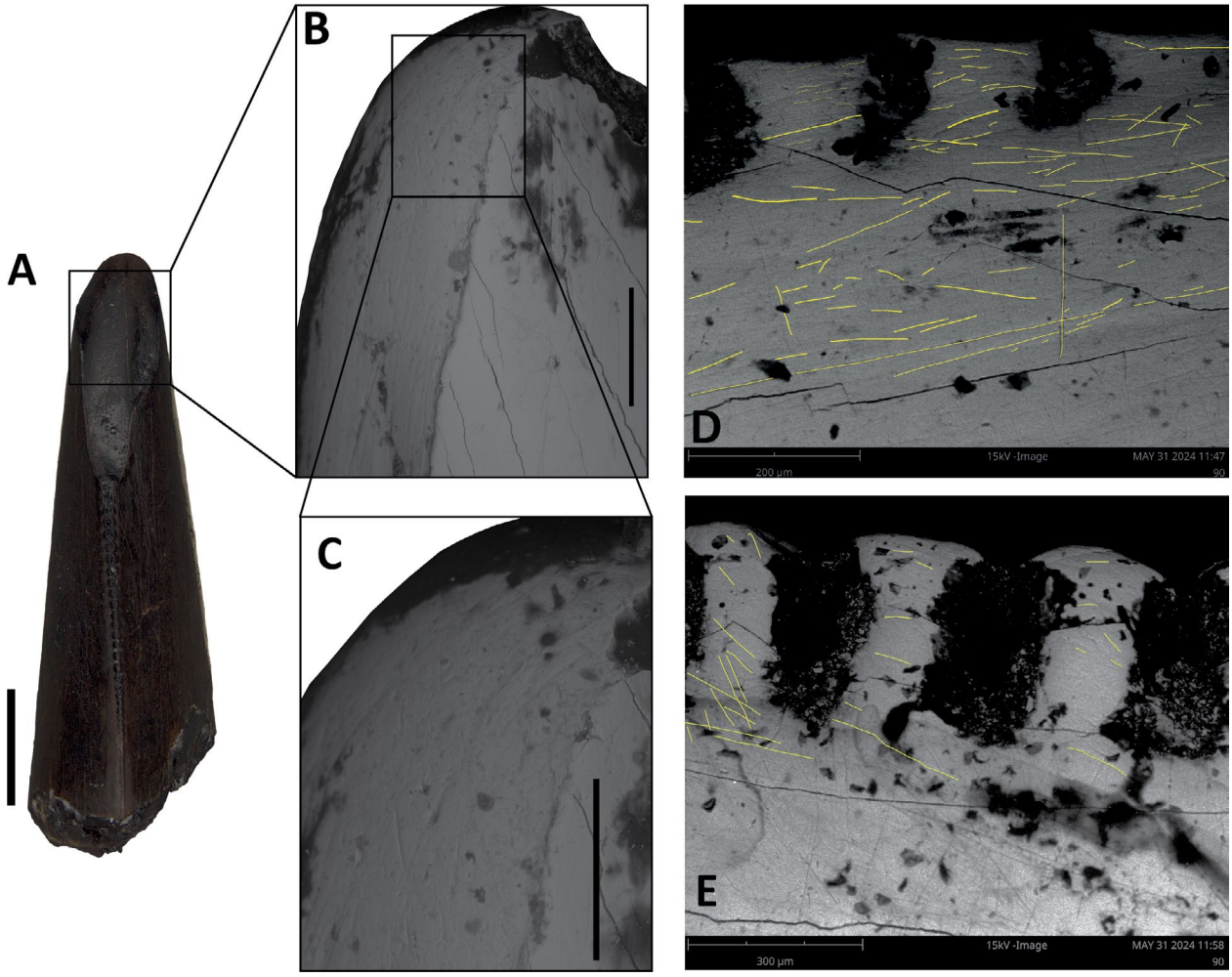


*Fig. 5.* Specimen MNHN/UL.AND.26. A, crown in mesial view. B, C, close views of the spalled surface on the SEM. D, detail of the scratches on the apical mesial denticles on the SEM. E, detail of the scratches on the central distal denticles on the SEM. Scale bars: 2 mm (A), 500 µm (B), 300 µm (C).

by sediment. Only near the base of the tooth it is possible to observe small, parallel, and faint striations on the denticles.

In the most apical denticles of the distal carina, the surface is covered by sediment; however, in some of them, parallel and oblique striations are still visible (Fig. 5E). This pattern is also present in some mid-crown denticles. Towards the base, around mid-crown height, some denticles lack their distal margin and appear to have been affected by abrasion, resulting in concavities that are filled with sediment. This abraded distal margin is also present on some basal denticles. Associated with these denticles, oblique striations can be observed, which are also present in the basalmost denticles.

*MNHN/UL.AND.213.* – This specimen was interpreted as a mesial crown of an indeterminate Coelurosauria (Malafaia *et al.* in review) (Table 1). The apex of the tooth crown is completely missing due to the presence of a prominent wear surface, which gives the crown a rounded apical end (Fig. 6A, B). This wear surface extends to the distal margin of the crown, forming a shallow concavity. The concavity is filled with sediment, making it impossible to observe any additional wear structures within it. The apical wear surface also slightly extends onto the mesial margin of the crown. This apical margin of the wear surface displays a high density of striations (Fig. 6B), predominantly oriented mesiodistally, although oblique striations with different orientations

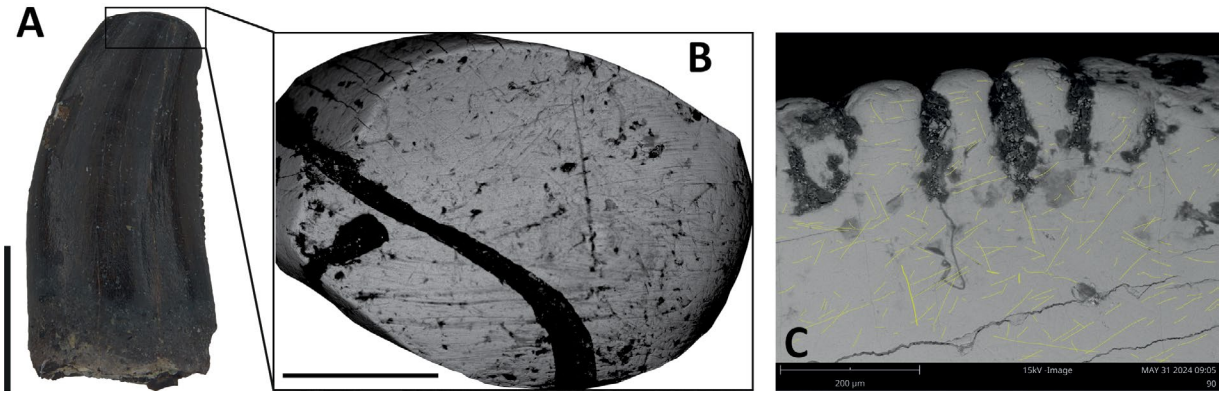


*Fig. 6.* Specimen MNHN/UL.AND.213. A, crown in labial view. B, detail of the wear surface in apical view on the SEM. C, detail of the scratches on the apical distal denticles on the SEM. Scale bars: 2 mm (A), 500 µm (B).

are also present. In lateral view, the two most apical preserved distal denticles are very abraded (Fig. 6C), apparently being the extension of the wear surface along the distal carina. This wear results in another concavity along the apical end of the distal carina, which is also filled with sediment. Other denticles also present evidence of wear, mostly expressed as irregularities along their distal margin. Along the distal margin of the crown, as well as on some denticles and adjacent to their base, oblique and parallel striations are observed (Fig. 6C).

*MNHN/UL.AND.206.* – This specimen (Fig. 7A) was interpreted as a lateral crown attributed to a juvenile *Allosaurus* (Malafaia *et al.* in review). The tooth crown is largely covered by sediment on both lingual and labial surfaces, including the denticles, which makes it difficult to observe any wear structures. However, some striations are visible near the apex of the crown on both distal (Fig. 7B) and mesial (Fig. 7C) denticles. On the denticles, most striations are parallel to the distal margin of the crown, but there are also a few oblique striations that are longer and deeper in some denticles. Some mesial denticles also evince striations, which are smaller and oriented obliquely and parallel to the mesial margin.

*MNHN/UL.AND.208.* – This specimen was interpreted as a lateral crown attributed to a velociraptorine dromaeosaurid (Malafaia *et al.* in review) (Table 1). The tooth crown does not present any wear surfaces (Fig. 7D). However, there is a high density of striations in the apical region of the crown and on the apical denticles of the distal carina (Fig. 7E), visible on both labial and lingual surfaces. Based on the identified striation patterns, two distinct sets can be distinguished: one with a parallel (to subparallel) orientation relative to the distal margin of the crown, and another with an oblique orientation. In the latter, striations are notably long, wide, and deep. The same striation pattern is present towards the base of the crown, including the central denticles of the distal carina (Fig. 7F). Some apical denticles of the distal carina appear abraded, presenting small concavities in their distal margin or having highly irregular ends, visible from both lingual and labial views. These most apical denticles of the distal carina are smaller than those in the central and basal sections of the crown and appear to be slightly affected by wear. Some denticles around mid-crown height also present concavities in their distal margins. Most of the labial surface of the crown is covered by sediment, but some irregularities are visible, probably also resulting from wear. Wear patterns are also present on the mesial serration of the crown, revealing some abrasion marks and striations, which are difficult to observe due to the small size of the denticles.

*MNHN/UL.AND.209.* – This specimen was interpreted as a mesial crown of an indeterminate Neocoelurosauria (Malafaia *et al.* in review) (Table 1). The apex of the crown is missing, and the most apical preserved part is fractured (Fig. 7G). The enamel is also poorly preserved, with several fractures and exposing the dentine in some parts. Additionally, large portions of the crown surface are covered by sediment, making the observation of wear features even more difficult. In the most apical preserved part of the crown, near a fractured surface, the enamel displays some striations with random patterns and orientations. Along the mesial crenulation of the crown, although less abundant, striations parallel to the mesial margin are present. In the most apical preserved denticles of the distal carina, small striations with parallel (to subparallel)

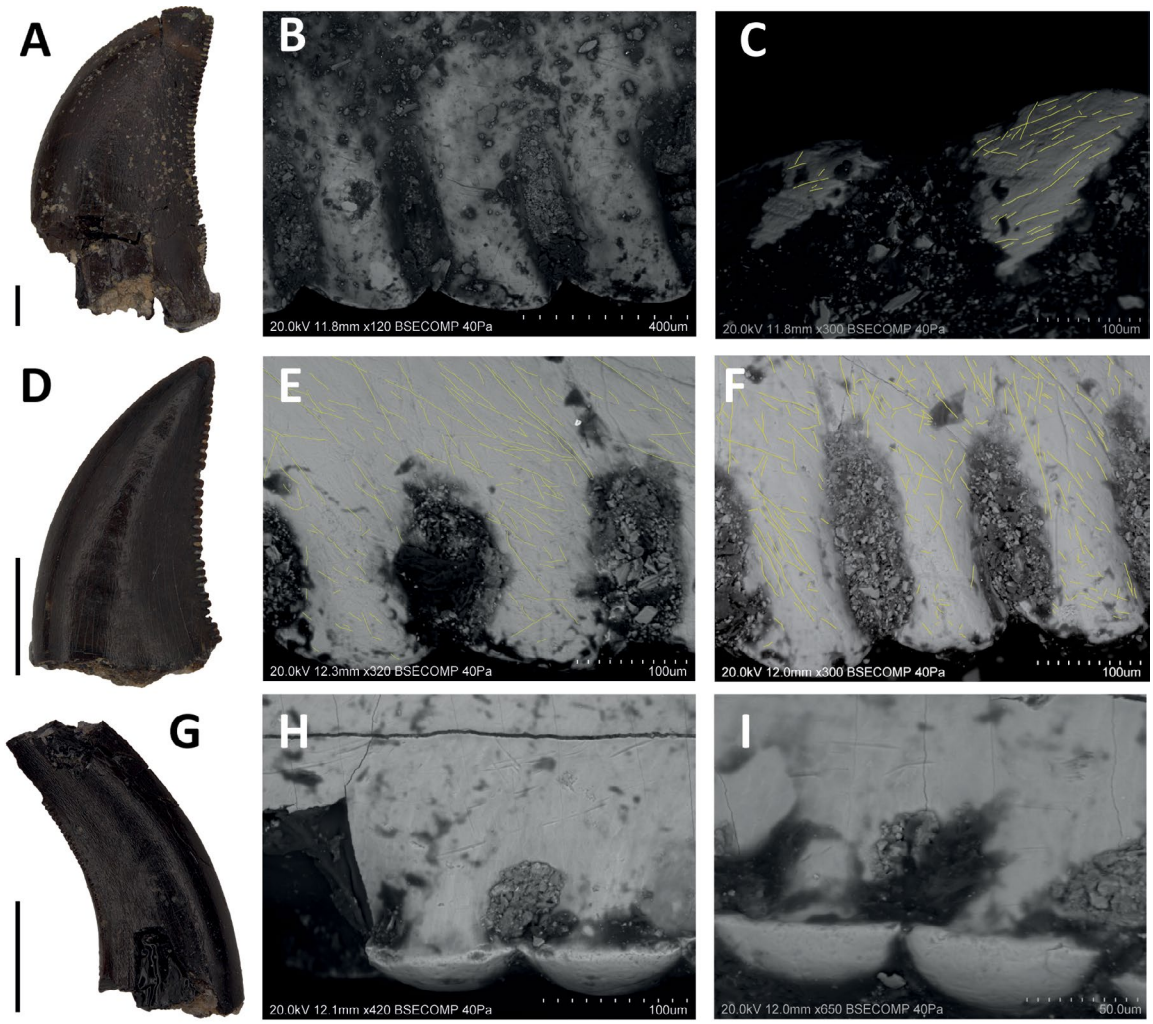


*Fig. 7.* Specimens presenting no wear surfaces. A, MNHN/UL.AND.206 in labial view. B, detail of the scratches on the apical distal denticles of MNHN/UL.AND.206 on the SEM. C, detail of the scratches on the apical mesial denticles of MNHN/UL.AND.206 on the SEM. D, MNHN/UL.AND.208 in lingual view. E, F, detail of the scratches on the apical and central distal denticles, respectively, on the SEM. G, MNHN/UL.AND.209 in lingual view. H, I, detail of the distal denticles of MNHN/UL.AND.209 showing few scratches on SEM. Scale bars: 2 mm.

orientations can also be observed, although they are not present in all denticles (Fig. 7H, I). Additionally, the unusual morphology of the denticles, which have a rounded external surface with a well-marked lateral border surrounding the apex of the denticle, may also be related to wear. Near the base of the denticles, oblique striations are present. Although several denticles are broken or covered with sediment, some mid-crown denticles exhibit both oblique and parallel striations. The labial surface of the crown is poorly preserved, with more fractures and missing parts than the lingual surface. Furthermore, it is also covered with sediment, making observations particularly challenging. Due to the lingual deflection of the carina, only four distal denticles are visible on the lingual surface, and no striations were observed. The distal margin is almost completely covered by sediment. However, some parallel striations are visible adjacent to the mesial margin of the crown.

## *Finite Element Analysis*

The model of MNHN/UL.AND.208 exhibits the lowest average and minimum stress values between 45° and 60°, with stress values gradually increasing as the angle deviates from this interval (Fig. 8; Table 3). The model's tooth displayed the highest stress values on the distal carina, where the force was applied. Lower

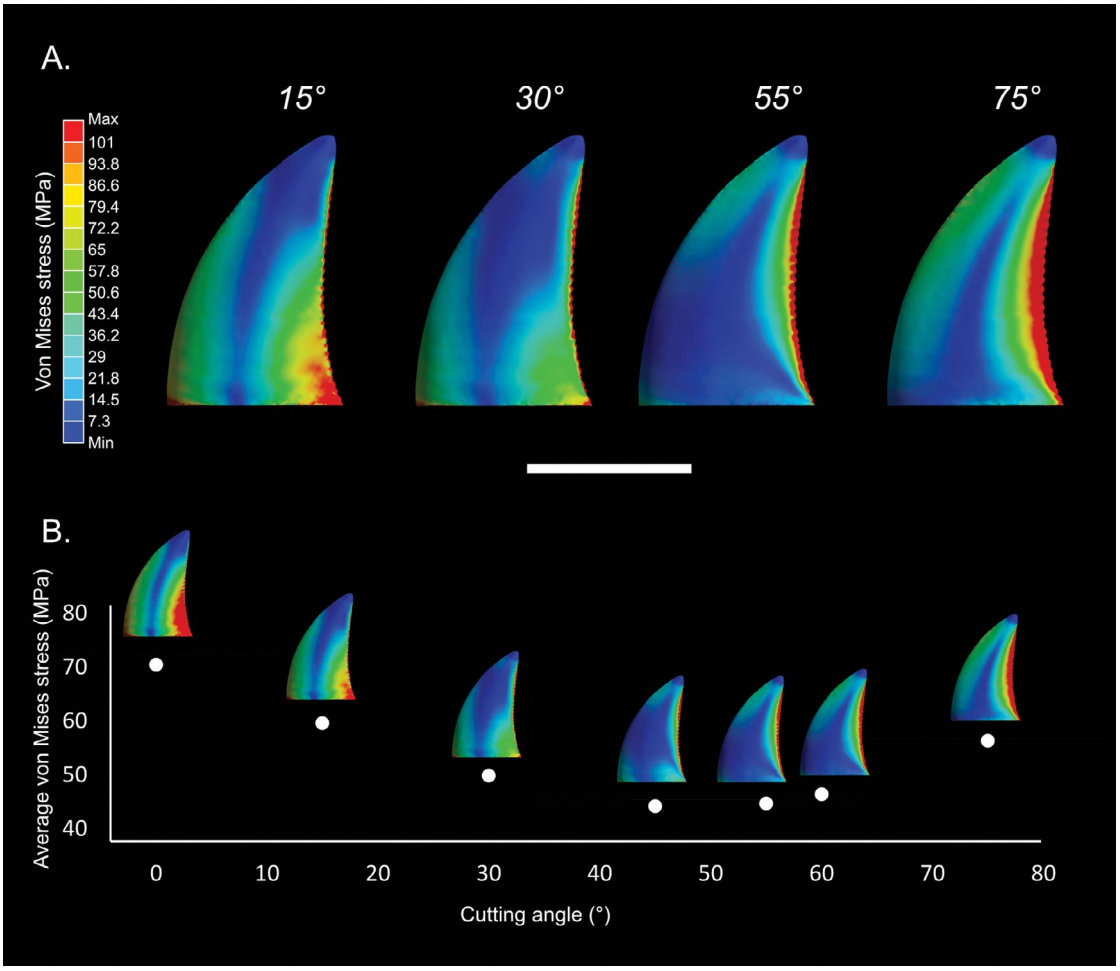


*Fig. 8.* Results of the Finite Element Analyses performed in the Dromaeosauridae (cf. Velociraptorinae) tooth (MNHN/UL.AND.208) showing Von Mises stress for the different cutting angles tested (A) and average von Mises stress (MPa) experienced by the tooth related with its Von Mises contour plots depending on the cutting angle scenario tested (B). Scale bar: 3 cm.

*Table 3.* Results of the Finite Element Analyses under the different cutting angle scenarios

| Angle (°) | Minimum (Mpa) | Maximum (Mpa) | Average (Mpa) |
|---|---|---|---|
| 0 | 0,096554 | 1062,3 | 70,445 |
| 15 | 0,06374 | 1032,2 | 59,629 |
| 30 | 0,027049 | 1125,1 | 49,834 |
| 45 | 0,005755 | 1278 | 44,2 |
| 55 | 0,0062882 | 1386,2 | 44,658 |
| 60 | 0,0076237 | 1426,2 | 46,388 |
| 75 | 0,012719 | 1484,9 | 56,315 |

stress values were observed on the distal carina, especially at non-optimal angles (outside the 45° - 60° range). However, the tooth body does not display any areas with high stress values (Fig. 8).

# Discussion

## *Wear surfaces and microwear interpretation*

The study of wear patterns on tooth crowns can provide valuable insights into diet and feeding mechanisms, independent of variations in tooth and denticle morphologies, tooth and body size, and phylogenetic context (Torices *et al.* 2018). However, the study of these structures in theropod teeth is still in its early stages. To assess the presence of wear surfaces on the teeth, this study applies the subjective wear classes defined by Farlow & Brinkman (1994), which categorize the degree of wear on each tooth as follows: 1) little or no wear; 2) slight to moderate wear, extending less than half the length of the carina; 3) extensive wear, extending more than half the length of the carina; and 4) wear that cannot be determined due to poor preservation or post-shedding breakage.

MNHN/UL.AND.208 and MNHN/UL.AND.206 fall into the class 1, as their crowns are well preserved and show no visible evidence of wear to the naked eye. Dental wear of this class is proposed to result from premature breaking of the teeth from the jaw, possibly during a fight or feeding (Farlow & Brinkman 1994). In contrast, the crown of MNHN/UL.AND.209 is too poorly preserved to determine the degree or the wear type (corresponding to class 4).

The crown of MNHN/UL.AND.212 exhibits a prominent wear surface extending onto the labial side from the most apical part of the preserved fragment and reaching about half its length (corresponding to class 3). It also presents long striations oriented parallel to the long axis of the wear surface, which are clearly visible to the naked eye. Lambe (1917) documented wear surfaces on the lingual and labial surfaces of lateral teeth of tyrannosaurs, interpreting them as the result of contact between opposing teeth during biting (Farlow & Brinkman 1994). This would have resulted in significant wear on the lingual surface of upper jaw teeth and the labial surface of lower jaw teeth. If this pattern is applied to the specimen from Andrés, it would suggest that this tooth belongs to the lower jaw, as the wear surface is located on the labial surface. This wear surface is elongated and elliptical in shape, extending into the dentine and with an orientation following the long axis of the tooth. Its edge is positioned next to the mesial margin, and it is located on the labial surface of the crown, resembling the wear/attritional facet described in some tyrannosaurid teeth (Schubert & Ungar 2005). In these specimens, some striations were also identified within the wear facets, which are usually visible to the naked eye and consistently oriented at about 15 degrees to the long axis of the facet (Schubert & Ungar 2005).

This pattern is similar to that found within the wear surface of MNHN/UL.AND.212, which also presents a consistent orientation of the scratches, with approximately 17 degrees from the long axis of the facet. While Molnar (1998) suggested that this type of wear surfaces may result from the contact between the tooth and the food, Schubert & Ungar (2005) argued that the consistent, parallel striations within the wear facet are more compatible with an attritional origin, caused by dental occlusion and vertically-oriented movement during biting. If the wear patterns found in these tyrannosaurid teeth are extrapolated to other theropod groups, the wear facet in MNHN/UL.AND.212 would be interpreted as resulting from dental occlusion of opposing teeth (Farlow & Brinkman 1994; Schubert & Ungar 2005; Candeiro *et al.* 2017) (Table 4). On the lingual surface of this tooth, another wear surface is observed, which appears to have a different aetiology. It is short, sub-quadrangular, and located in the apical region of the crown (class 2, *sensu* Farlow & Brinkman 1994). Although no striation pattern could be identified due to sediment covering the surface, it appears shallower than the wear surface described on the labial surface. The apical margin of this surface is irregular and approximately perpendicular to the long axis of the crown. This morphology is consistent with the definition provided by Schubert & Ungar (2005) for a spalled surface, interpreted as resulting from repeated contact between the tooth and the food during food processing (Table 4). Other authors suggested that these spalled surfaces could be a consequence of crushing bones or other hard materials (Candeiro *et al.* 2017). Schubert & Ungar (2005) noted that wear facets do not occur on both the labial and lingual sides of a single tooth. As there is a wear facet on the labial side of MNHN/UL.AND.212, the surface on the lingual side must have a different origin and is therefore interpreted as a spalled surface (*sensu* Schubert & Ungar 2005).

The wear surface observed in MNHN/UL.AND.26, (class 2, *sensu* Farlow & Brinkman 1994), located at the apex and extending across all surfaces of the crown with rounded and irregular edges, is similar to the spalled surface described in a tyrannosaurid lateral tooth (Schubert & Ungar 2005). In this specimen, the wear surface is shallow, resembling the spalled surface found on the lingual side of MNHN/UL.AND.212. Schubert & Ungar (2005) noted that wear striations within spalled surfaces are typically microscopic and heterogeneously oriented. In MNHN/UL.AND.26, only a few striations are present within the wear surface, and these are barely visible. Therefore, the wear surface in this specimen is also interpreted as resulting from antemortem enamel spalling due to repeated contact between the tooth and the food (possibly including the crushing of hard elements such as bones) (Table 3).

The wear surface on MNHN/UL.AND.213 (class 2, *sensu* Farlow & Brinkman 1994) is markedly different from all those previously described. It occurs at the apex of the tooth, which is entirely worn, resulting in a rounded top surface with several clearly visible striations. Both the edges of this structure, as well as the surface itself are rounded and appear somewhat polished. A surface with a similar morphology was described in a pliosauroid tooth and interpreted as resulting from breakage of crown apex followed by subsequent wear of the surface (Massare 1987). Another type of tooth wear was described for some ichthyosaur species, where the crown forms a conical shape with a blunt apex and rough surface

*Table 4.* Morphology and respective interpretation of the different wear surfaces found in the studied specimens

| Specimen | Wear surfaces | Interpretation |
|---|---|---|
| MNHN/UL.AND.212 | 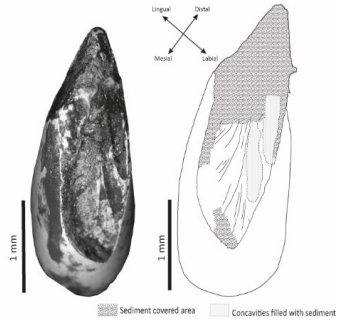 | Wear surface (*sensu* Schubert & Ungar 2005), resulting from the contact between opposite tooth rows. |
| | 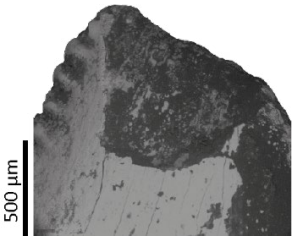 | Spalled surface (*sensu* Schubert & Ungar 2005) resulting from the repeated contact between the tooth and the food. |
| MNHN/UL.AND.26 | 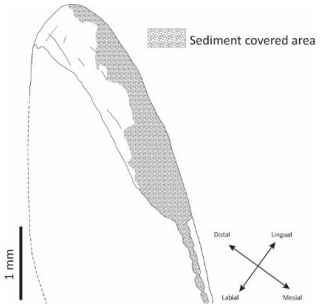 | Spalled surface (*sensu* Schubert & Ungar 2005), resulting from the repeated contact between the tooth and the food. |
| MNHN/UL.AND.213 | 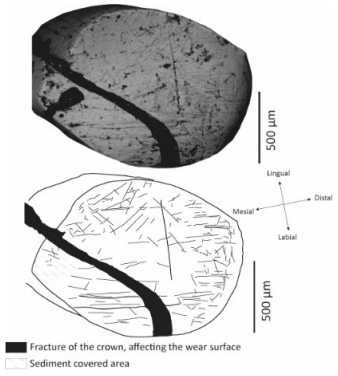 | Early breakage of the tooth crown apex and, subsequently worn down over time. |

(Massare 1987), similar to the 'tip-rounding' wear type described by Abler (1992) and Molnar (1998) for tyrannosaurs. Despite the taxonomic differences, when comparing the morphology of the unusual wear surface of MNHN/UL.AND.213 with these two types, several characteristics correspond closely to those described by Massare (1987) in the pliosauroid tooth. Furthermore, it seems unlikely that wear alone could cause such a pronounced surface and the complete absence of the crown apex. Given that this is a mesial tooth crown, it most probably had a grasping function (Massare 1987), which would have increased its susceptibility to breakage. Although D'Amore (2009) stating that mesial teeth contact the substrate only

when the jaw is nearly closed, a grasping function associated with mesial teeth could indicate, that these teeth would have been the first to contact with the prey, thereby increasing the probability of breakage. Such a break may have removed the entire tip of the tooth, which then remained functional and was progressively worn down over time (Table 4), resulting in a rounded surface and edges, and in the striations present on it (Massare 1987).

Regarding microwear patterns near the denticles, it is important to note that the angles further discussed were not only calculated using the formulae presented in the methodology for circular values, but also with the formulae for both simple arithmetic mean and standard deviation. This was necessary in order to allow comparisons with the results obtained by Torices et al. (2018), who treated them as linear values. However, the results obtained for the mean angle values do not differ significantly when using the circular or the linear formula (with the exception of the tooth MNHN/UL.AND.212).

In all of the studied teeth, four distinct sets of scratch orientations were identified: 1) the most abundant set, which comprises scratches obliquely oriented relative to the carina (averaging between 22º and 55º, see Table 2); 2) a less abundant set of oblique scratches, oriented almost perpendicularly to the first set (approximately 130º to 160º relative to the carina); 3) scratches parallel to the long axis of the tooth; and 4) a set of large, deeper scratches with random orientations. The second set of oblique scratches, although present near the denticles of all tooth crowns, is significantly less abundant than the other patterns. Therefore, the orientation of these structures was excluded from the statistical analysis. The fourth set of striations is characterized by being deeper, more pronounced, and sometimes wider and longer than the other identified scratches. These scratches often display random orientations and frequently overlap and intersect with other striation sets. Due to their appearance, random orientation, and distribution across the tooth crowns, these marks are interpreted as resulting from taphonomic processes. Although these striations are present in all studied specimens, and occasionally relatively abundant, they were not measured due to their inferred taphonomic origin. All scratches observed on the distal denticles of MNHN/UL.AND.206 fall into this category, as do the majority of scratches found on the denticles of MNHN/UL.AND.209 and MNHN/UL.AND.212.

The most abundant scratches identified in the studied specimens exhibit two preferential orientations: one oblique and the other approximately parallel to the carina. This pattern is similar to that observed in scratches associated with denticles of different theropod clades (Torices *et al.* 2018). The average orientation values range from 36º to 55º for MNHN/UL.AND.26, MNHN/UL.AND.208, and MNHN/UL.AND.213, which are the specimens for which measurements of eighty scratches were possible to obtain (following the methodology of Torices *et al.* 2018). The striations on these crowns are more commonly observed near the distal carina, although they are also associated with the mesial carina (when present). In all studied tooth crowns, oblique striations are more abundant than parallel ones. Parallel striations tend to be more commonly on the surface of the denticles rather than at their base. This pattern contrasts with that found in the teeth of other theropods, in which parallel scratches are generally more abundant than oblique ones (Torices *et al.* 2018). Regarding striation size, there does not seem to be any significant difference between the two orientation sets, although some crowns display longer oblique ones. For MNHN/UL.AND.209 and MNHN/UL.AND.212, the average orientation values also fall near the 36º to 55º range, although only eleven and twenty scratches, respectively, were measured. In MNHN/UL.AND.206, the average value is considerably lower. However, as only thirty-four scratches were measured, and exclusively near the mesial denticles, these data should be interpreted with caution.

## *Implications for the interpretation of feeding mechanisms in theropods*

The results obtained through FEA for MNHN/UL.AND.208 indicate that the optimal angle for tooth use lies between 45° and 60°, which aligns closely with the average angle of 55º observed for the oblique scratches on this tooth. These results suggest that this theropod was using its teeth at an optimal angle to minimize stress, reflected by the orientation of the oblique scratches and as demonstrated by the results of the FEA. This outcome is consistent with those reported by Torices *et al.* (2018) for other coelurosaurian theropods. Specifically, the Late Cretaceous coelurosaurian theropods Troodontidae indet. and *Saurornitholestes* also exhibit similar angles for both the optimal angle for stress minimisation and the predominant orientation of oblique scratches. Although the angle measured in the Late Jurassic tooth from Andrés is higher than the 30° measured for Troodontidae indet. and *Saurornitholestes* (Torices *et al.* 2018), it is comparable to the optimal angle of 45° reported on the Cretaceous noasaurid *Vespersaurus paranaensis* through FEA (Barbosa *et al.* 2023).

The pattern of scratch orientations, along with the FEA results obtained in this study, are compatible

with a puncture-and-pull feeding movement. This type of movement was first proposed by Huene (1923), who interpreted the presence of opisthocoelous anterior presacral vertebrae as an adaptation for the pulling movement in 'Megalosauridae', 'Deinodontidae' (Tyrannosauridae), and possibly *Ceratosaurus*. Since then, this feeding behaviour has been repeatedly hypothesized for theropods based on studies of jaw muscle insertion (Bakker 1986), neck muscle reconstruction (Snively & Russell 2007), tooth marks on bones (e.g. Erickson & Olson 1996) and, more recently, by combining wear facet analysis and FEA in coelurosaurian dinosaurs (Torices *et al.* 2018). This feeding mechanism is similar to that employed by the extant *Varanus komodoensis*, the Komodo dragon (e.g. Erickson & Olson 1996; D'Amore & Blumenschine 2009) and implies that the apex of the tooth would be the first part to get in contact with the prey's body. Due to the curvature of the crown, its mesial part would contact with the body before the distal one (D'Amore 2009), thereby supporting the highest resistance (Torices *et al.* 2018). As the tooth continued to penetrate the flesh, it would create a set of parallel scratches and subsequently, as the theropod closed its mouth and retracted its head away from the prey, the tooth would move obliquely through the flesh, producing more randomly oriented and oblique scratches.

Despite differences in denticle morphology among MNHN/UL.AND.26, MNHN/UL.AND.208, and MNHN/UL.AND.213, the same striation pattern was observed, possibly indicating a similar origin mechanism. Furthermore, MNHN/UL.AND.26 and MNHN/UL.AND.208 are interpreted as belonging to dromaeosaurids (Malafaia *et al.* in review), one of the theropod groups for which this feeding mechanism has previously been proposed (Torices *et al.* 2018). Since MNHN/UL.AND.213 (interpreted as belonging to Coelurosauria indet.) exhibits the same striation pattern, it is plausible that this individual employed a similar movement and feeding mechanism. As for the other three specimens, MNHN/UL.AND.212 also display a comparable pattern, although fewer scratches were counted, possibly due to obliteration by taphonomic processes and presence of sediment covering the enamel. Correlating this crown with the respective taxonomic classification, it also corresponds to a possible dromaeosaurid (Malafaia *et al.* in review), suggesting that the feeding mechanism could have been also similar to that previously mentioned. MNHN/UL.AND.206 and MNHN/UL.AND.209 are the crowns most affected by taphonomic processes, with fewer, but longer and deeper scratches, most of which are interpreted as of taphonomic origin. However, the parallel and oblique scratches observed on the mesial denticles of MNHN/UL.AND.206 (interpreted as possible belonging to a juvenile *Allosaurus*), correspond to the pattern described above for the puncture-and-pull movement, This interpretation is consistent with previous proposals for this taxon, which suggest that *Allosaurus* defleshed carcasses by retraction of the skull (Snively & Russel 2007; Snively *et al.* 2013; Torices *et al.* 2018; Winkler *et al.* 2022).

The use of the puncture-and-pull mechanism among different theropod groups from Andrés, including dromaeosaurids and other possible coelurosaurs, and *Allosaurus*, suggests the persistence of this feeding strategy over time, at least since the Late Jurassic, as was previously suggested based on other analyses (Winkler et al. 2022).

Based on FEA, Torices *et al.* (2018) found an optimal bite angle of 30° for a troodontid indet. and *Saurornitholestes*, while *Dromaeosaurus* exhibited similar stress across all bite angles. Additionally, the preferential orientation of the oblique scratches in these taxa ranged from 32.25° in coelurosaurs of uncertain affinity to 45.3° in an indeterminate large theropod, all from the Campanian-Maastrichtian of Spanish South Pyrenees. The dataset studied here indicates greater variability, with preferential oblique scratch orientations ranging from 22° in MNHN/UL.AND.206 to 55° in MNHN/UL.AND.208 and MNHN/UL.AND.212, along with an optimal bite angle between around 45° and 60° for MNHN/UL.AND.208. This greater variation may be related to the smaller sample size of this study compared to that of Torices *et al.* (2018), but it could also reflect differences in tooth function related to their position in the jaw, or even an evolutionary shift in tooth use and feeding strategies between Late Jurassic and Late Cretaceous theropod faunas.

## Conclusions

The principal goal of this work was to study the wear surfaces and other wear patterns on a sample of isolated theropod teeth collected from Upper Jurassic levels of the Andrés fossil site (Portugal) to analyse dietary habits and feeding mechanisms on these dinosaurs. This study allowed the identification of distinct wear surfaces as well as various macro- and microscopic striation patterns in different specimens. The diverse dental wear patterns are interpreted as having different origins, related to varied feeding behaviours and interactions with food. Extensive wear, sometimes cutting into the dentine, with regular margins observed in a dromaeosaurid crown, is interpreted as

resulting from tooth-to-tooth contact. More superficial wear with irregular margins, sometimes observed in different positions of the tooth crown, is interpreted as spalled surfaces, resulting from repeated contact between the tooth and the food, or as a consequence of crushing hard elements. A mesial tooth exhibits an unusual and very extensive wear surface, interpreted as the result of breakage followed by subsequent wear, consistent with a grasping function and a high probability of breakage during feeding. The crowns that showed no wear surfaces are interpreted as having broken prematurely from the jaw.

The results of the FEA performed on the Dromaeosauridae (cf. Velociraptorinae) tooth indicate that the optimal bite angle aligns with the orientation of the abundant oblique scratches identified, which is consistent with findings from Late Cretaceous Coelurosauria. This suggests an optimal use of the teeth to minimize stress. The microwear striation patterns (mainly oblique and parallel to the carinae) are compatible with a puncture-and-pull feeding mechanism, similar to that observed in the extant Komodo dragon and inferred for several Late Jurassic and Late Cretaceous theropods. This hypothesis is also supported by the FEA results obtained in this study.

This study emphasizes the importance of analysing dental wear structures to enhance our understanding of theropod feeding strategies and ecology. Despite being limited to a few clades, this study provides valuable data that can be useful for further research on this subject, allowing comparisons between different patterns and feeding strategies across various groups. Future studies incorporating a larger phylogenetic and/or stratigraphical sample will provide a more comprehensive understanding of the variations observed between the teeth studied here from the Late Jurassic of Portugal and those previously published from the Late Cretaceous of Canada and Spain.

*Acknowledgments.*- We thank José Amorim for access and assistance during field work, Pedro Dantas as a co-director of the project, the Museu Nacional de História Natural e da Ciência, in particular to Judite Alves, Roberto Keller, and Liliana Póvoas for access to the collections and equipment necessary to the measurement and photographs of the fossils, to the HERCULES Laboratory for access to the SEM, to Instituto Superior Técnico, especially to Manuel Francisco Costa Pereira for access to the microtomographer and assistance to obtain the 3D model of the tooth, and the Geological Museum, in particular to Jorge Sequeira and Rúben Dias for access to the collections. Finally, we also thank Dragonfly for the free licence provided. This project was supported by the Fundação para a Ciência e a Tecnologia / Instituto Dom Luiz, through a PhD grant (UI/BD/154498/2022) and the CEECIND/01770/2018 individual contract (https://doi.org/10.54499/CEECIND/01770/2018/CP1534/CT0004), as well as by FCT I.P./MCTES through national funds (PIDDAC) – UIDB/50019/2020 (https://doi.org/10.54499/UIDB/50019/2020), UIDP/50019/2020 (https://doi.org/10.54499/UIDP/50019/2020) and LA/P/0068/2020 (https://doi.org/10.54499/LA/P/0068/2020).

## References

Abler, W.L. 1992: The serrated teeth of tyrannosaurid dinosaurs, and biting structures in other animals. *Paleobiology 18*, 161–183.

Azerêdo, A.C., Cabral, M.C., Martins, M.J., Loureiro, I.M. & Inês, N. 2010: Estudo estratigráfico dum novo afloramento da Formação de Cabaços (Oxfordiano) na região da Serra do Bouro (Caldas da Rainha). *Comunicações Geológicas 97*, 5–22.

Bakker, R.T. 1986: *The Dinosaur Heresies*. William Morrow and Company, New York.

Barbosa, G.G., Langer, M.C., Martins, N.d.O. & Montefeltro, F.C. 2023: Assessing the palaeobiology of *Vespersaurus paranaensis* (Theropoda, Noasauridae), Cretaceous, Bauru Basin – Brazil, using Finite Element Analysis. *Cretaceous Research 150*, 105594. https://doi.org/10.1016/j.cretres.2023.105594

Candeiro, C.R.A., Currie, P.J., Candeiro, C.L. & Bergqvist, L.P. 2017: Tooth wear and microwear of theropods from the late Maastrichtian Marília Formation (Bauru Group), Minas Gerais state, Brazil. *Earth and Environmental Science Transactions of the Royal Society of Edinburgh 106*, 229–233. https://doi.org/10.1017/S175569101600013X

Creech, J.E. 2004: *Phylogenetic Character Analysis of Crocodylian Enamel Microstructure and Its Relevance to Biomechanical Performance*. Unpublished Master thesis, Florida State University, Tallahassee.

D'Amore, D.C. 2009: A Functional Explanation for Denticulation in Theropod Dinosaur Teeth. *The Anatomical Record 292*, 1297–1314. https://doi.org/10.1002/ar.20977

D'Amore, D.C. & Blumenschine, R.J. 2009: Komodo monitor (*Varanus komodoensis*) feeding behaviour and dental function reflected through tooth marks on bone surfaces, and the application to ziphodont paleobiology. *Paleobiology 35*, 525–552. http://dx.doi.org/10.1666/0094-8373-35.4.525

Dantas, P., Pérez-Moreno, B.P., Chure, D.J., Silva, C.M., Santos, V.F., Póvoas, L., Cachão, M., Sanz, J.L., Pires, C., Bruno, G., Ramalheiro, G. & Carvalho, A.M.G. 1999: O Dinossáurio Carnívoro *Allosaurus fragilis* no Jurássico Superior português. *Al-Madan 8*, 23–28.

Erickson, G.M. & Olson, K.H. 1996: Bite marks attributable to *Tyrannosaurus rex*: preliminary description and implications. *Journal of Vertebrate Paleontology 16*, 175–178. http://dx.doi.org/10.1080/02724634.1996.10011297

Farlow, J.O. & Brinkman, D.L. 1994: Wear Surfaces on the Teeth of Tyrannosaurs. *The Paleontological Society Special Publications 7*, 165–176. https://doi.org/10.1017/S2475262200009503

Fisher, N.I. 1993: *Statistical Analysis of Circular Data*. Cambridge University Press, Cambridge. https://doi.org/10.1017/CBO9780511564345

Fürsich, F.T., Schneider, S., Werner, W., Lopez-Mir, B. & Pierce, C.S. 2022: Life at the continental–marine interface: palaeoenvironments and biota of the Alcobaça Formation (Late Jurassic, Central Portugal), with a formal definition of the unit appended. *Palaeobiodiversity and Palaeoenvironments 102*, 265–329. https://doi.org/10.1007/s12549-021-00496-x

Hendrickx, C., Mateus, O. & Araújo, R. 2015: A proposed terminology of theropod teeth (Dinosauria, Saurischia). *Journal of Vertebrate Paleontology 35*, e982797. https://doi.org/10.1080/02724634.2015.982797

Huene, F. 1923: Carnivorous Saurischia in Europe since the Triassic. *Bulletin of the Geological Society of America 34*, 449–458. https://doi.org/10.1130/GSAB-34-449

Kubo, T., Kubo, M.O., Sakamoto, M., Winkler, D.E., Shibata, M., Zheng, W., Jin, X. & You, H.L. 2023: Dental microwear texture analysis reveals a likely dietary shift within Late Cretaceous ornithopod dinosaurs. *Palaeontology 66*, e12681. https://doi.org/10.1111/pala.12681

Kullberg, J.C., Rocha, R.B., Soares, A.F., Rey, J., Terrinha, P., Azerêdo, A.C., Callapez, P., Duarte, L.V., Kullberg, M.C., Martins, L., Miranda, R., Alves, C., Mata, J., Madeira, J., Mateus, O., Moreira, M. & Nogueira, C.R. 2013: A Bacia Lusitaniana:

Estratigrafia, Paleogeografia e Tectónica, 195–347. *In* Dias, R., Araújo, A., Terrinha, P. & Kullberg, J.C. (Eds), *Geologia de Portugal, Vol II, Geologia Mesocenozoica de Portugal*, Escolar Editora, Lisboa.

Lambe, L.M. 1917: The Cretaceous theropodous dinosaur Gorgosaurus. *Memoir, Geological Survey of Canada 100*, 84 p. https://doi.org/10.4095/101672

Lautenschlager, S. 2017: Functional niche partitioning in Therizinosauria provides new insights into the evolution of theropod herbivory. *Palaeontology 60*, 375–387. https://doi.org/10.1111/pala.12289

Lautenschlager, S., Witmer, L.M., Altangerel, P. & Rayfield, E.J. 2013: Edentulism, beaks, and biomechanical innovations in the evolution of theropod dinosaurs. *Proceedings of the National Academy of Sciences 110*, 20657–20662. https://doi.org/10.1073/pnas.1310711110

Lautenschlager, S., Brassey, C.A., Button, D.J. & Barrett, P.M. 2016: Decoupled form and function in disparate herbivorous dinosaur clades. *Scientific Reports 6*, 26495. https://doi.org/10.1038/srep26495

Malafaia, E., Ortega, F., Escaso, F., Dantas, P., Pimentel, N., Gasulla, J.M., Ribeiro, B., Barriga, F. & Sanz, J.L. 2010: Vertebrate fauna at the *Allosaurus* fossil-site of Andrés (Upper Jurassic), Pombal, Portugal. *Journal of Iberian Geology 36*, 193–204. http://dx.doi.org/10.5209/rev_JIGE.2010.v36.n2.7

Manuppella, G. 1974: *Carta Geológica de Portugal, folha 23-A (Pombal). Escala 1: 50 000* (1ª ed.). Serviços Geológicos de Portugal, Lisboa.

Manuppella, G., Zbyszewski, G. & Ferreira, O.V. 1978: *Notícia Explicativa da Carta Geológica de Portugal, folha 23-A (Pombal). Escala 1: 50 000* (1ª ed.). Serviços Geológicos de Portugal, Lisboa, 62 p.

Massare, J.A. 1987: Tooth morphology and prey preference of Mesozoic marine reptiles. *Journal of Vertebrate Paleontology 7*, 121–137. http://dx.doi.org/10.1080/02724634.1987.10011647

Molnar, R.E. 1998: Mechanical factors in the design of the skull of *Tyrannosaurus rex* (Osborn, 1905). *Gaia: Revista de Geociências* 15, 193–218.

Molnar, R.E. & Farlow, J.O. 1990: Carnosaur paleobiology, 222–234. *In* Weishampel, D.B., Dodson, P. & Osmólska, H. (Eds), *The Dinosauria*, University of California Press, Berkeley.

Moreno, K., Wroe, S., Clausen, P., McHenry, C., D'Amore, D.C., Rayfield, E.J. & Cunningham, E. 2008: Cranial performance in the Komodo dragon (*Varanus komodoensis*) as revealed by high-resolution 3-D finite element analysis. *Journal of Anatomy 212*, 736–746. http://dx.doi.org/10.1111/j.1469-7580.2008.00899.x

Ősi, A., Apesteguía, S. & Kowalewski, M. 2010: Non-avian theropod dinosaurs from the early Late Cretaceous of central Europe. *Cretaceous Research 31*, 304–320. http://dx.doi.org/10.1016/j.cretres.2010.01.001

Ősi, A., Barrett, P.M., Földes, T. & Tokai, R. 2014: Wear pattern, dental function, and jaw mechanism in the Late Cretaceous ankylosaur *Hungarosaurus*. *The Anatomical Record 297*, 1165–1180. https://doi.org/10.1002/ar.22910

Paula, F.V. & Carvalho, T.S. 2024: Dados circulares: tratamento, análise e uma aplicação a dados reais. *Conexões - Ciência E Tecnologia 18*, e022019. https://doi.org/10.21439/cone xoes.v18i0.3300

Pérez-Moreno, B.P., Chure, D.J., Pires, C., Silva, C.M., Santos, V.F., Dantas, P., Póvoas, L., Cachão, M., Sanz, J.L. & Carvalho, A.M.G. 1999: On the presence of *Allosaurus fragilis* (Theropoda: Carnosauria) in the Upper Jurassic of Portugal: first evidence of an intercontinental dinosaur species. *Journal of the Geological Society 156*, 449–452.

Pimentel, N.L. 2009: Contextualização paleogeográfica das jazidas de vertebrados do Jurássico Superior da Bacia Lusitânica. *Paleolusitana 1*, 465–470.

Rivals, F. & Deniaux, B. 2003: Dental microwear analysis for investigating the diet of an argali population (*Ovis ammon antiqua*) of mid-Pleistocene age, Caune de l'Arago cave, eastern Pyrenees, France. *Palaeogeography, Palaeoclimatology, Palaeoecology 193*, 443–455. https://doi.org/10.1016/S0031-0182(03)00260-8

Sakaki, H., Winkler, D.E., Kubo, T., Hirayama, R., Uno, H., Miyata, S., Endo, H., Sasaki, K., Takisawa, T. & Kubo, M.O. 2022: Non-occlusal dental microwear texture analysis of a titanosauriform sauropod dinosaur from the Upper Cretaceous (Turonian) Tamagawa Formation, northeastern Japan. *Cretaceous Research 136*, 105218. https://doi.org/10.1016/j.cretres.2022.105218

Schubert, B.W. & Ungar, P.S. 2005: Wear facets and enamel spalling in tyrannosaurid dinosaurs. *Acta Palaeontologica Polonica 50*, 93–99.

Schulz, E., Calandra, I. & Kaiser, T.M. 2013: Feeding ecology and chewing mechanics in hoofed mammals: 3D tribology of enamel wear. *Wear 300*, 169–179. http://dx.doi.org/10.1016/j.wear.2013.01.115

Schulz-Kornas, E. & Winkler, D.E. 2023: A comprehensive overview of wear analysis in life history evolution. *96th Annual Meeting of the German Society for Mammalian Biology*, Zurich.

Scott, R.S., Ungar, P.S., Bergstrom, T.S., Brown, C.A., Grine, F.E., Teaford, M.F. & Walker, A. 2005: Dental microwear texture analysis shows within-species diet variability in fossil hominins. *Nature 436*, 693–695. https://doi.org/10.1038/nature03822

Skutschas, P.P, Gvozdkova, V.A., Averianov, A.O., Lopatin, A.V., Martin, T., Schellhorn, R., Kolosov, P.N., Markova, V.D., Kolchanov, V.V., Grigoriev, D.V., Kuzmin, I.T. & Vitenk, D.D. 2021: Wear patterns and dental functioning in an Early Cretaceous stegosaur from Yakutia, Eastern Russia. *PLoS One 16*, e0248163. https://doi.org/10.1371/journal.pone.0248163

Snively, E. & Russell, A.P. 2007: Functional morphology of neck musculature in the Tyrannosauridae (Dinosauria, Theropoda) as determined via a hierarchical inferential approach. *Zoological Journal of the Linnean Society 151*, 759–808. https://doi.org/10.1111/j.1096-3642.2007.00334.x

Snively, E., Cotton, J.R., Ridgely, R. & Witmer, L.M. 2013: Multibody dynamics model of head and neck function in *Allosaurus* (Dinosauria, Theropoda). *Palaeontologia Electronica 16*, 1–29. https://doi.org/10.26879/338

Teixeira, C., França, J.C., Zbyszewski, G., Ferreira, O.V. & Manuppella, G. 1966: *Carta Geológica de Portugal, folha 23-C (Leiria). Escala 1: 50 000* (1ª ed.). Serviços Geológicos de Portugal, Lisboa.

Therrien, F., Henderson D.M. & Ruff, C.B. 2005: Bite me: Biomechanical models of theropod mandibles and implications for feeding behavior, 179–237. *In* Carpenter, K. (ed): *The Carnivorous Dinosaurs*, Indiana University Press, Bloomington.

Torices, A., Wilkinson, R., Arbour, V.M., Ruiz-Omeñaca, J.I. & Currie, P.J. 2018: Puncture-and-pull biomechanics in the teeth of predatory coelurosaurian dinosaurs. *Current Biology 28*, 1467–1474. https://doi.org/10.1016/j.cub.2018.03.042

Ungar, P.S., Merceron, G. & Scott, R.S. 2007: Dental microwear texture analysis of Varswater bovids and early Pliocene paleoenvironments of Langebaanweg, Western Cape Province, South Africa. *Journal of Mammalian Evolution 14*, 163–181. http://dx.doi.org/10.1007/s10914-007- 9050-x

Williamson, T.E. & Brusatte, S.L. 2014: Small theropod teeth from the Late Cretaceous of the San Juan Basin, northwestern New Mexico and their implications for understanding latest Cretaceous dinosaur evolution. *PLoS One 9*, e93190. https://doi.org/10.1371/journal.pone.0093190

Winkler, D.E., Kubo, T., Kubo, M.O., Kaiser, T.M. & Tütken, T. 2022: First application of dental microwear texture analysis to infer theropod feeding ecology. *Palaeontology 65*, e12632. https://doi.org/10.1111/pala.12632

Withnell, C. & Ungar, P. 2014: A preliminary analysis of dental microwear as a proxy for diet and habitat in shrews. *Mammalia 78*, 409–415. https://doi.org/10.1515/mammalia-2013- 0121